Carrier Frequency Offset Estimation in Uplink OFDMA Systems: An Approach Relying on Sparse Recovery

Min Huang, Lei Huang, *Senior Member, IEEE*, Chongtao Guo, Peichang Zhang, Jihong Zhang, and Lie-Liang Yang, *Fellow, IEEE*

Abstract—This paper proposes a novel blind carrier frequency offset (CFO) estimator, namely the sparse recovery assisted CFO (SR-CFO) estimator, for the uplink orthogonal frequency-division multiple access (OFDMA) systems. By exploiting the sparsity embedded in the OFDMA data, the CFO estimation is formulated as an optimization problem of sparse recovery with high-resolution. Meanwhile, in order to enhance the estimation accuracy of CFOs, background noise and sampling errors are mitigated by exploiting the structure of the noise covariances matrix in the transformed observation data, and the asymptotic distribution of the sampling errors. Furthermore, we propose an approach for deriving the regularization parameter used by the SR-CFO estimator, so as to control the tradeoff between the data fitting error and the sparsity of solution. The performance of the proposed SR-CFO estimator along with other four existing estimators is investigated and compared. Numerical results show that the proposed SR-CFO estimator is superior to the state-of-the-art estimators in terms of the estimation reliability.

Index Terms—OFDMA, carrier frequency offset, estimator, sparse recovery.

I. INTRODUCTION

In wireless communications, orthogonal frequency-division multiplexing (OFDM) has been widely employed to support the downlink and uplink transmissions, and to support multiuser communications via assigning different subcarriers to different users, forming the orthogonal frequency division multiple access (OFDMA). In OFDMA systems, the achievable performance is very sensitive to the carrier frequency offsets (CFOs) induced by the mismatch between transceiver oscillators. CFOs lead to strong multiple-access interference (MAI), which may significantly degrade the system performance if it is not

M. Huang, L. Huang, C. Guo, P. Zhang, and J. Zhang are with the College of Information Engineering, Shenzhen University, Shenzhen 518060, China (e-mail: mhuang@szu.edu.cn; lhuang@szu.edu.cn; ctguo@szu.edu.cn; zpc1029384756@hotmail.com; zhangjh@szu.edu.cn).

L.-L. Yang is with the School of Electronics and Computer Science, University of Southampton, Southampton SO17 1BJ ,U.K. (e-mail: lly@ecs.soton.ac.uk).

effectively mitigated. Hence, in practical systems, the CFOs need to be estimated with sufficient accuracy which are then compensated or used for MAI mitigation.

In literature, maximum likelihood algorithm [1] and its variant versions [2], [3] have been proposed for estimation of the CFOs in OFDMA systems. The common drawbacks of these methods are the high implementation complexity and the requirement of pilots, which reduces the attainable spectral efficiency. In order to combat these problems, a blind CFO estimation scheme has been proposed in [4]. Specially, by exploiting the periodic structure of the received signals in the interleaved OFDMA uplink systems, the multiple signal classification approach referred to as MUSIC has been adopted in [4] to estimate the CFOs. It is shown in [4] that the MUSIC algorithm has a low computational complexity, and is capable of achieving a good estimation performance. However, when the CFOs of the signals from different users are close to each other in the frequency domain, and when the signal-to-noise ratio (SNR) is relatively low, it is usually hard to separate the CFOs by the MUSIC approach. Furthermore, in order to identify the CFOs, the MUSIC approach has to resort to a highly involved spectral searching procedure, which is rather computationally intensive. Due to these issues, the MUSIC estimator has been replaced by the estimators designed based on the rotational invariance technique, such as the ESPRIT [5]. Moreover, in order to further reduce the computational complexity, an improved ESPRIT, namely the Unitary-ESPRIT, has been proposed in [6] for estimation of CFOs. More recently, a unitary subspace improved minimum output variance (U-SIMOV) estimator has been introduced in [7] for CFO estimation. By combining the unitary transformation with the subspace projection technique, the U-SIMOV is able to improve the CFO estimation performance of the Unitary-ESPRIT, provided that the CFOs with respect to different users are sufficiently separated from each other.

In order to attain high-resolution estimations for the closely located CFOs, especially, in low SNR region, we propose a novel CFO estimator in this paper, with the main contributions as follows.

1) A novel CFO estimation algorithm designed based on the sparse recovery is proposed in this paper, which is referred to as the sparse recovery assisted CFO (SR-CFO) estimator. Our high-resolution CFO estimator is formulated as a sparse optimization problem without relying on requiring pilots. Furthermore, with the aid of the Lagrangian duality theory [8], [9], an approach is proposed for deriving the regularization parameter required by our SR-CFO estimator.

2) A selection matrix is designed for mitigating the effect of additive Gaussian noise by exploiting the structure of the noise variances in the transformed observation data.

3) A whitening filter is designed for coping with the sampling errors by exploiting the asymptotic distribution of the sampling errors.

4) The performance of our SR-CFO estimator is investigated by simulations, which is also compared with four existing CFO estimators. Our studies and simulation results show that the proposed SR-CFO estimator outperforms all the benchmark CFO estimators by providing a higher resolution and also a higher

estimation accuracy. Furthermore, the regularization parameter derived by our proposed approach is nearly optimum in the sense of minimum mean-square error (MSE).

II. SYSTEM MODEL

We consider an interleaved N-subcarrier OFDMA uplink system, where the N subcarriers are evenly divided into Q subchannels, each of which includes $P = N/Q$ subcarriers. Assume that there are K $(K \leq Q)$ users active in the system and each of the active users is assigned one subchannel. For the k-th user, where $k \in \{0, \cdots, K - 1\}$, its symbol vector $[x_0^{(k)}, \cdots, x_{P-1}^{(k)}]^T \in \mathbb{C}^P$ to be transmitted is mapped to its assigned subchannel, namely the $q^{(k)}$-th subchannel, composed of the P subcarriers with the indices constituting a set $\boldsymbol{\phi}^{(k)} = \{q^{(k)}, q^{(k)} + Q, \cdots, q^{(k)} + (P - 1)Q\}$, where $q^{(k)}$ is lowest index of the subcarriers assigned to user k.

Assume a multipath slow fading channel, whose fading coefficients can be assumed to be constant during one OFDMA symbol duration. Then, the channel frequency response on the $\phi_p^{(k)}$-th subcarrier of user k can be expressed as [4]

$$h_p^{(k)} = \sum_{l=0}^{L^{(k)}-1} \alpha_l^{(k)} e^{-j2\pi \phi_p^{(k)} \Delta_f \tau_l^{(k)}} \tag{1}$$

where $L^{(k)}$ is the number of multipath taps of the fading channel from user k to the base station (BS), Δ_f represents the subcarrier spacing between two adjacent subcarriers, $\alpha_l^{(k)}$ and $\tau_l^{(k)}$ denote the channel gain and time delay of the l-th tap, respectively. Note that $\phi_p^{(k)}$ is the p-th element of $\boldsymbol{\phi}^{(k)}$ and $\phi_p^{(k)} = q^{(k)} + pQ$ for $p = 0, 1, \cdots, P - 1$.

At the receiver, after sampling and removal of the cyclic prefix (CP), the time-domain signals received from the k-th user in the absence of noise can be expressed as

$$r^{(k)}(n) = \sum_{p=0}^{P-1} h_p^{(k)} x_p^{(k)} e^{j2\pi(\phi_p^{(k)} + \varepsilon^{(k)})\Delta_f n T_s}$$

$$= \sum_{p=0}^{P-1} h_p^{(k)} x_p^{(k)} e^{j(2\pi/N)(\phi_p^{(k)} + \varepsilon^{(k)})n}, \ n = 0, \cdots, N - 1 \tag{2}$$

where $T_s = 1/(N\Delta_f)$ denotes the sampling period and $\varepsilon^{(k)} \in (-0.5, 0.5)$ is the CFO normalized by Δ_f. It can be shown [5] that $\{r^{(k)}(n)\}_{n=0}^{N-1}$ have the property of

$$r^{(k)}(n + mP) = e^{j2\pi m \theta^{(k)}} r^{(k)}(n) \tag{3}$$

where $\theta^{(k)} \triangleq (q^{(k)} + \varepsilon^{(k)})/Q$ is referred to as the effective CFO. Explicitly, given $q^{(k)}$ and Q, $\theta^{(k)}$ is a function of $\varepsilon^{(k)}$. Hence, we can estimate $\theta^{(k)}$ instead of estimating $\varepsilon^{(k)}$.

As the BS receives signals simultaneously from K active users, the received signals can be expressed as

$$\Upsilon(n) = \sum_{k=0}^{K-1} r^{(k)}(n) + z(n), \ n = 0, \cdots, N - 1 \tag{4}$$

where $z(n)$ is the Gaussian noise distributed with mean zero and variance σ^2. In order to exploit the periodicity existing in $\{r^{(k)}(n)\}_{n=0}^{N-1}$, the N received signals can be arranged as $\Upsilon = [\mathbf{r}(0), \cdots, \mathbf{r}(P - 1)] \in \mathbb{C}^{Q \times P}$, where $\mathbf{r}(i) = [\Upsilon(i), \Upsilon(i + P), \cdots, \Upsilon(i + (Q - 1)P)]^T \in \mathbb{C}^Q$.

It follows that Υ can be expressed as

$$\Upsilon = VS + Z \tag{5}$$

where $V = [a(\theta^{(0)}), \cdots, a(\theta^{(K-1)})] \in \mathbb{C}^{Q \times K}$ with $a(\theta^{(i)}) = [e^{j2\pi\theta^{(i)}0}, \cdots, e^{j2\pi\theta^{(i)}(Q-1)}]^T \in \mathbb{C}^Q$, $S = [r^{(0)}, \cdots, r^{(K-1)}]^T \in \mathbb{C}^{K \times P}$ with $r^{(i)} = [r^{(i)}(0), \cdots, r^{(i)}(P - 1)]^T \in \mathbb{C}^P$, and $Z = [z(0), \cdots, z(P - 1)] \in \mathbb{C}^{Q \times P}$ is the corresponding noise matrix with $z(i) = [z(i), z(i + P), \cdots, z(i + (Q - 1)P)]^T \in \mathbb{C}^Q$. Our objective is to estimate the effective CFOs of $\theta^{(k)}$ for $k = 0, \cdots, K - 1$, which are embedded in V, based on (5).

III. SR-CFO ESTIMATION ALGORITHM

A. CFO Estimation Based on Sparse Recovery

According to (3), and remembering that $\varepsilon^{(k)} \in (-0.5, 0.5)$, the effective CFO of the k-th active user is distributed in the range of $((q^{(k)} - 0.5)/Q, (q^{(k)} + 0.5)/Q)$. Considering that $q^{(k)} \in \{0, 1, \cdots, Q - 1\}$, we can readily know that the effective CFOs of the K active users are sparsely distributed in the range of $(-0.5/Q, 1 - 0.5/Q)$. Thus, by invoking all the possible effective CFOs, Υ in (5) can be rewritten in a high-resolution and sparse representation as

$$\Upsilon = \bar{V}\bar{S} + Z \tag{6}$$

where $\bar{V} = [a(\bar{\theta}^{(0)}), \cdots, a(\bar{\theta}^{(\bar{K}-1)})] \in \mathbb{C}^{Q \times \bar{K}}$ and the set of $\{\bar{\theta}^{(0)}, \cdots, \bar{\theta}^{(\bar{K}-1)}\}$ gives a sampling grid of all possible effective CFOs, while $\bar{S} = [\bar{r}^{(0)}, \cdots, \bar{r}^{(\bar{K}-1)}]^T \in \mathbb{C}^{\bar{K} \times P}$ with $\bar{r}^{(i)} = [\bar{r}^{(i)}(0), \cdots, \bar{r}^{(i)}(P - 1)]^T \in \mathbb{C}^P$. In general, we have $\bar{K} \gg K$. Hence, $\bar{S}$ is a row sparse matrix, whose i-th row is nonzero and equals to the corresponding row of S in (5), only when there truly exists an effective CFO of $\bar{\theta}^{(i)}$ having a value in $(-0.5/Q, 1 - 0.5/Q)$. Consequently, the problem of effective CFO estimation based on (5) is equivalent to identifying the positions of the nonzero rows in $\bar{S}$ seen in (6). In principle, this problem may be directly solved by the $\ell_{2,0}$-norm compressive sensing algorithms [10]. However, the non-convexity of $\ell_{2,0}$-norm algorithms leads to high computational complexity. Alternatively, the $\ell_{2,0}$-norm can be approximated by the $\ell_{2,1}$-norm [11], which may be solved with relatively low complexity. However, the approximation error may be large, especially in the case that the ℓ_2-norms of the nonzero rows in $\bar{S}$ have significantly different values. In order to circumvent these problems, and with the aid of the idea from [9], below we make use of the covariance matrix of the received signals of (6) as the new observations, based on which the effective CFOs are estimated. Note that, since in this case only the 2nd order moments are required, which allow us to efficiently suppress the effect from the additive Gaussian noise and the sampling errors. Eventually, better recovery performance can be achieved, as shown in Section IV.

To begin with, the sampling covariance matrix of $\mathbf{\Upsilon}$ of (6) can be derived and expressed as

$$\hat{\mathbf{R}} = \bar{\mathbf{V}} \mathbf{R}_s \bar{\mathbf{V}}^H + \mathbf{R}_n + \mathbf{E} \tag{7}$$

which is a $(Q \times Q)$-dimensional matrix. In (7), $\mathbf{R}_s = \mathbb{E}[\bar{\mathbf{S}}\bar{\mathbf{S}}^H] = \mathrm{diag}\{P\sigma_{\bar{r}(0)}^2, \cdots, P\sigma_{\bar{r}(\bar{K}-1)}^2\}$ with $\sigma_{\bar{r}(k)}^2 = \mathbb{E}[\bar{r}^{(k)}(n)\bar{r}^{(k)}(n)^H]$ being the power received from the k-th user, $\mathbf{R}_n = \mathrm{diag}\{P\sigma^2, \cdots, P\sigma^2\}$ is the noise covariance matrix, while $\mathbf{E}$ reflects the error between the covariance matrix of $\mathbf{\Upsilon}$ given in (6), which is $\bar{\mathbf{V}}\mathbf{R}_s\bar{\mathbf{V}}^H + \mathbf{R}_n$, and its sampling covariance matrix $\hat{\mathbf{R}}$ of (7). Let us vectorize (7), yielding a Q^2-length vector [12]

$$\mathbf{y} \triangleq \mathrm{vec}\{\hat{\mathbf{R}}\} = \mathbf{\mathscr{V}}\boldsymbol{\varsigma} + \boldsymbol{\rho} + \boldsymbol{\xi} \tag{8}$$

where $\mathbf{\mathscr{V}} \triangleq \bar{\mathbf{V}}^* \odot \bar{\mathbf{V}}$, $\boldsymbol{\varsigma} \triangleq [P\sigma_{\bar{r}(0)}^2, \cdots P\sigma_{\bar{r}(\bar{K}-1)}^2]^T$, $\boldsymbol{\rho} \triangleq \mathrm{vec}(\mathbf{R}_n) = [P\sigma^2\mathbf{e}_1^T, \cdots, P\sigma^2\mathbf{e}_Q^T]^T$ and $\boldsymbol{\xi} \triangleq \mathrm{vec}(\mathbf{E})$. Here, $(\cdot)^*$, $\odot$ and $\mathbf{e}_i$ denote, respectively, the complex conjugate, Khatri-Rao product [12], and the i-th column of the identity matrix $\mathbf{I}_Q$. Based on (8), our CFO estimation problem is converted to a problem of identifying the locations of nonzero elements in $\boldsymbol{\varsigma}$.

From (8) we know that there are Q nonzero elements in the noise resulted component of $\boldsymbol{\rho}$, whose positions are known. Therefore, they can be canceled by deleting the corresponding elements in $\mathbf{y}$ but at the cost of the loss of Q degrees of freedom (DOFs). In mathematical form, the cancellation of the noise resultant components in (8) can be implemented by pre-multiplying a selection matrix $\mathbf{J} \in \mathbb{R}^{Q(Q-1) \times Q^2}$ satisfying $\mathbf{J}\boldsymbol{\rho} = \mathbf{0}$ on $\mathbf{y}$, yielding

$$\mathbf{u} \triangleq \mathbf{J}\mathbf{y} = \mathbf{J}\mathbf{\mathscr{V}}\boldsymbol{\varsigma} + \mathbf{J}\boldsymbol{\xi} \tag{9}$$

Note that, according to the structure of $\mathbf{e}_i$, $\mathbf{J}$ can be constructed from the identity matrix $\mathbf{I}_{Q^2}$ by removing its $\{0 \times Q + 1, 1 \times Q + 2, \cdots, (Q-1) \times Q + Q\}$ rows.

According to [13], $\boldsymbol{\xi}$ is asymptotically complex normal ($\mathcal{CN}$) distributed, if P is sufficiently large. In this case, the distribution of $\boldsymbol{\xi}$ can be approximated as $\boldsymbol{\xi} \sim \mathcal{CN}(\mathbf{0}, (\hat{\mathbf{R}}^T \otimes \hat{\mathbf{R}})/P)$, where $\otimes$ denotes the Kronecker product [12]. Therefore, $\mathbf{J}\boldsymbol{\xi}$ in (9) follows the distribution of $\mathcal{CN}(\mathbf{0}, \mathbf{G})$ with $\mathbf{G} \triangleq (\mathbf{J}(\hat{\mathbf{R}}^T \otimes \hat{\mathbf{R}})\mathbf{J}^T)/P$. Explicitly, the transformed noise $\mathbf{J}\boldsymbol{\xi}$ is colored, which may lead to severe performance degradation. In order to alleviate its effect, we may whiten $\mathbf{J}\boldsymbol{\xi}$ through multiplying $\mathbf{u}$ of (9) by $\mathbf{G}^{-\frac{1}{2}}$, yielding

$$\hat{\mathbf{u}} \triangleq \mathbf{G}^{-\frac{1}{2}}\mathbf{u} = \mathbf{\Psi}\boldsymbol{\varsigma} + \boldsymbol{\nu} \tag{10}$$

where $\mathbf{\Psi} \triangleq \mathbf{G}^{-\frac{1}{2}}\mathbf{J}\mathbf{\mathscr{V}}$ and $\boldsymbol{\nu} \triangleq \mathbf{G}^{-\frac{1}{2}}\mathbf{J}\boldsymbol{\xi} \sim \mathcal{CN}(\mathbf{0}, \mathbf{I}_{Q(Q-1)})$ is now a white Gaussian noise vector.

With the aid of the above preparation, finally, the optimization problem for finding the nonzero elements in $\boldsymbol{\varsigma}$ can be described as

$$\min_{\boldsymbol{\varsigma}} \left\{ \frac{1}{2} \|\hat{\mathbf{u}} - \mathbf{\Psi}\boldsymbol{\varsigma}\|_2^2 + h \|\boldsymbol{\varsigma}\|_1 \right\}, \quad \text{s.t. } \boldsymbol{\varsigma} \succeq \mathbf{0} \tag{11}$$

where $h \geq 0$ is a regularization parameter for controlling the contribution between the ℓ_2-norm and ℓ_1-norm, i.e., between the data fitting error and the sparsity of the solution [14]. In (11), the ℓ_1-norm is used for approximating the ℓ_0-norm for the purpose of constructing a convex optimization problem. However, from (8) we know that the nonzero elements in $\boldsymbol{\varsigma}$ represent the power received from the different users, which may be very different. In this case, as shown in [15], a large approximation error may occur. In order to cope with this problem, we propose to estimate the effective CFOs by solving an alternative optimization problem described as

$$\min_{\boldsymbol{\varsigma}} \left\{ \frac{1}{2} \|\hat{\mathbf{u}} - \mathbf{\Psi}\boldsymbol{\varsigma}\|_2^2 + h \sum_{i=0}^{\bar{K}-1} w_i |\varsigma_i| \right\}, \quad \text{s.t. } \boldsymbol{\varsigma} \succeq \mathbf{0} \tag{12}$$

where ς_i denotes the i-th element of $\boldsymbol{\varsigma}$ and w_i is the corresponding weight applied to guarantee that $w_i\varsigma_i \leq 1$. According to the analysis in [15], [16], we have $\varsigma_i \leq P/(\bar{\mathbf{v}}_i^H \hat{\mathbf{R}}^{-1} \bar{\mathbf{v}}_i)$. Therefore, we can choose w_i to have a value of $w_i = (\bar{\mathbf{v}}_i^H \hat{\mathbf{R}}^{-1} \bar{\mathbf{v}}_i)/P$, where $\bar{\mathbf{v}}_i$ represents the i-th column of $\bar{\mathbf{V}}$. However, as shown in (12), the estimation performance is also dependent on the value of the regularization parameter h, which needs to be set appropriately. Below we address in detail the regularization parameter setting.

B. Regularization Parameter Setting

The value of h in (12) plays an important role for the achievable estimation performance. In particular, a small value of h may incur many spurious effective CFOs, while a large value of h may yield a large estimation error. Hence, it is important to set h to a suitable value. In this section, we derive h based on (12) with the aid of the Lagrangian duality [8], [9], which is near optimum as demonstrated in Section IV.

First, let us rewrite (12) as an optimization problem associated with the constraints as

$$\min_{\boldsymbol{\varsigma}} \left\{ \frac{1}{2} \|\boldsymbol{\nu}\|_2^2 + h \sum_{i=0}^{\bar{K}-1} w_i |\varsigma_i| \right\} \text{ s.t. } \boldsymbol{\nu} = \hat{\mathbf{u}} - \mathbf{\Psi}\boldsymbol{\varsigma}, \ \boldsymbol{\varsigma} \succeq \mathbf{0}. \tag{13}$$

Then, with the aid of the *Lagrangian multipliers*, the corresponding unconstrained minimization problem can be described as

$$\min_{\boldsymbol{\varsigma}, \boldsymbol{\nu}} \left\{ \frac{1}{2} \|\boldsymbol{\nu}\|_2^2 + h \sum_{i=0}^{\bar{K}-1} w_i |\varsigma_i| + \boldsymbol{\mu}^T(\boldsymbol{\nu} - \hat{\mathbf{u}} + \mathbf{\Psi}\boldsymbol{\varsigma}) - \boldsymbol{\lambda}^T\boldsymbol{\varsigma} \right\} \tag{14}$$

where $\boldsymbol{\mu}$ and $\boldsymbol{\lambda} \succeq \mathbf{0}$ are respectively the *Lagrange multipliers* for the constraints of $\boldsymbol{\nu} = \hat{\mathbf{u}} - \mathbf{\Psi}\boldsymbol{\varsigma}$ and $\boldsymbol{\varsigma} \succeq \mathbf{0}$. It can be shown that, for a fixed $\boldsymbol{\varsigma}$, the minimization of (14) over $\boldsymbol{\nu}$ results in

$$\boldsymbol{\mu} = -\boldsymbol{\nu} = -(\hat{\mathbf{u}} - \mathbf{\Psi}\boldsymbol{\varsigma}). \tag{15}$$

Upon substituting (15) into (14) to eliminate the variable $\boldsymbol{\nu}$, we obtain the minimization problem in terms of $\boldsymbol{\varsigma}$ as

$$\min_{\boldsymbol{\varsigma}} \left\{ -\frac{1}{2} \|\boldsymbol{\mu}\|_2^2 - \boldsymbol{\mu}^T\hat{\mathbf{u}} + h \sum_{i=0}^{\bar{K}-1} w_i |\varsigma_i| + \boldsymbol{\mu}^T\mathbf{\Psi}\boldsymbol{\varsigma} - \boldsymbol{\lambda}^T\boldsymbol{\varsigma} \right\} \tag{16}$$

Furthermore, according to the Lagrangian duality [8], the minimization problem of (13) is equivalent to the maximization problem of

$$\max_{\boldsymbol{\mu}, \boldsymbol{\lambda}} \left\{ -\tfrac{1}{2} \|\boldsymbol{\mu}\|_2^2 - \boldsymbol{\mu}^T \hat{\boldsymbol{u}} + \inf_{\boldsymbol{\varsigma}} \left[h \sum_{i=0}^{\bar{K}-1} w_i |\varsigma_i| + \boldsymbol{\mu}^T \boldsymbol{\Psi} \boldsymbol{\varsigma} - \boldsymbol{\lambda}^T \boldsymbol{\varsigma} \right] \right\}$$
(17)

where $\inf_{\boldsymbol{\varsigma}} \left[f(\boldsymbol{\varsigma}, \boldsymbol{\mu}, \boldsymbol{\lambda}) \right]$ represents the minimum of $f(\boldsymbol{\varsigma}, \boldsymbol{\mu}, \boldsymbol{\lambda})$ over $\boldsymbol{\varsigma}$ for given $\boldsymbol{\mu}$ and $\boldsymbol{\lambda}$. Then, by exploiting the *Karush-Kuhn-Tucker* condition [8], we should have $\boldsymbol{\lambda}^T \boldsymbol{\varsigma} = 0$ in (17). Consequently, the term of $\inf_{\boldsymbol{\varsigma}} \left[h \sum_{i=0}^{\bar{K}-1} w_i |\varsigma_i| + \boldsymbol{\mu}^T \boldsymbol{\Psi} \boldsymbol{\varsigma} - \boldsymbol{\lambda}^T \boldsymbol{\varsigma} \right]$ in (17) can be written as $\sum_{i=0}^{\bar{K}-1} \inf_{\varsigma_i}[\beta_i]$, where $\beta_i \overset{\Delta}{=} hw_i |\varsigma_i| + \eta_i \varsigma_i$ with η_i being the i-th element of $\boldsymbol{\mu}^T \boldsymbol{\Psi}$, i.e., $\eta_i = \boldsymbol{\psi}_i^T \boldsymbol{\mu} = -\boldsymbol{\psi}_i^T (\hat{\boldsymbol{u}} - \boldsymbol{\Psi} \boldsymbol{\varsigma})$. Here, $\boldsymbol{\psi}_i$ represents the i-th column of $\boldsymbol{\Psi}$. In order to determine $\inf_{\varsigma_i}[\beta_i]$, let us express β_i in detail as

$$\beta_i = \begin{cases} hw_i \varsigma_i + \eta_i \varsigma_i, & \text{if } \varsigma_i \geq 0 \\ -hw_i \varsigma_i + \eta_i \varsigma_i, & \text{if } \varsigma_i < 0 \end{cases}.$$
(18)

From (18), we can readily know that β_i achieves its minimum of 0, i.e., $\inf_{\varsigma_i}[\beta_i] = 0$, under the condition of $hw_i + \eta_i \geq 0$ when $\varsigma_i \geq 0$, or under the condition of $-hw_i + \eta_i < 0$ when $\varsigma_i < 0$. Under all other conditions, $\inf_{\varsigma_i}[\beta_i] = -\infty$. Therefore, we have

$$\inf_{\varsigma_i}[\beta_i] = \begin{cases} 0, & \text{if } hw_i \geq |\eta_i| \\ -\infty, & \text{otherwise} \end{cases}$$
(19)

However, $\inf_{\varsigma_i}[\beta_i] = -\infty$ is meaningless for an optimization problem. Hence, we should have the constraint on h as

$$hw_i \geq |\eta_i| = \sqrt{\boldsymbol{\psi}_i^T (\hat{\boldsymbol{u}} - \boldsymbol{\Psi} \boldsymbol{\varsigma})(\boldsymbol{\psi}_i^T (\hat{\boldsymbol{u}} - \boldsymbol{\Psi} \boldsymbol{\varsigma}))^H},$$
$$i = 0, \cdots, \bar{K} - 1$$
(20)

As shown previously in association with (10), $\hat{\boldsymbol{u}} - \boldsymbol{\Psi} \boldsymbol{\varsigma} \sim \mathcal{CN}(0, \boldsymbol{I}_{Q(Q-1)})$. Hence, we have $\boldsymbol{\psi}_i^T (\hat{\boldsymbol{u}} - \boldsymbol{\Psi} \boldsymbol{\varsigma}) \sim \mathcal{CN}(0, \boldsymbol{\psi}_i^T \boldsymbol{\psi}_i^*)$, from which we can readily know that

$$\sqrt{2/(\boldsymbol{\psi}_i^T \boldsymbol{\psi}_i^*)} \boldsymbol{\psi}_i^T (\hat{\boldsymbol{u}} - \boldsymbol{\Psi} \boldsymbol{\varsigma}) \sim \mathcal{CN}(0, 2).$$
(21)

Equation (21) implies that both the real and imaginary parts of $\sqrt{2/(\boldsymbol{\psi}_i^T \boldsymbol{\psi}_i^*)} \boldsymbol{\psi}_i^T (\hat{\boldsymbol{u}} - \boldsymbol{\Psi} \boldsymbol{\varsigma})$ are independently Gaussian distributed with the distribution of $\mathcal{N}(0, 1)$. Therefore, the square of $\sqrt{2/(\boldsymbol{\psi}_i^T \boldsymbol{\psi}_i^*)} \boldsymbol{\psi}_i^T (\hat{\boldsymbol{u}} - \boldsymbol{\Psi} \boldsymbol{\varsigma})$ follows the central χ^2-distribution with two DOFs, which can be expressed as

$$(2/(\boldsymbol{\psi}_i^T \boldsymbol{\psi}_i^*)) \boldsymbol{\psi}_i^T (\hat{\boldsymbol{u}} - \boldsymbol{\Psi} \boldsymbol{\varsigma})(\boldsymbol{\psi}_i^T (\hat{\boldsymbol{u}} - \boldsymbol{\Psi} \boldsymbol{\varsigma}))^H \sim \chi^2(2)$$
(22)

where $\chi^2(D)$ stands for the χ^2-distribution with D DOFs.

Let us assume that P_γ is a probability close to one. Then, we can find a corresponding value γ satisfying

$$\text{Pr}(\mathcal{X}^2(2) \leq \gamma) = P_\gamma$$
(23)

With the aid of (20) and (22), (23) can be written as

$$\text{Pr}\left(2/(\boldsymbol{\psi}_i^T \boldsymbol{\psi}_i^*) |\eta_i|^2 \leq \gamma\right) = \text{Pr}\left(|\eta_i| \leq \frac{\sqrt{\boldsymbol{\psi}_i^T \boldsymbol{\psi}_i^*}}{\sqrt{2}} \sqrt{\gamma}\right) = P_\gamma$$
(24)

Therefore, if we choose

$$hw_i \geq \frac{\sqrt{\boldsymbol{\psi}_i^T \boldsymbol{\psi}_i^*}}{\sqrt{2}} \sqrt{\gamma} \text{ or } h \geq \frac{\sqrt{\boldsymbol{\psi}_i^T \boldsymbol{\psi}_i^*}}{\sqrt{2} w_i} \sqrt{\gamma}$$
(25)

then, the constraint of $hw_i \geq |\eta_i|$ in (20) can be satisfied with a probability of at least P_γ. Consequently, by considering all the $\bar{K}$ constraints in (20), h can be chosen as

$$h = \left(\max_i \left\{ \frac{\|\boldsymbol{\psi}_i\|_2}{\sqrt{2} w_i} \right\} \right) \sqrt{\gamma}.$$
(26)

Finally, after substituting h obtained from (26) into (12), we can then estimate the effective CFOs by solving the optimization problem, which can be achieved by many existing optimization packages, e.g., the SeDuMi [17].

Note that, the computational complexity of the proposed SR-CFO estimation algorithm is mainly contributed by solving (12). When the SeDuMi package is used, it requires at least $\mathcal{O}(\bar{K}^3 Q(Q-1))$ complex multiplications according to [18]. This complexity is higher than that of some existing algorithms, e.g., the Unitary-ESPRIT [6], which has the complexity of $\mathcal{O}(PQ^2)$. However, as shown in the next section, the estimation performance of our proposed algorithm is better than that of the existing algorithms.

IV. SIMULATION RESULTS

In this section, we evaluate the achievable performance of our proposed SR-CFO estimation algorithm and also compare it with some existing algorithms, when an uplink QPSK-OFDMA system is considered. In the considered OFDMA system, the available bandwidth is divided into 1024 subcarriers with the minimum spacing of 11.16 kHz. In order to avoid inter symbol interference (ISI), a CP of length 64 is employed. We assume that the time-varying channels for all the active users have the same number of taps of $L^{(k)} = 10$, and that the mean power of the taps follows an exponential distribution [5], [7]. In detail, the mean power of the l-th tap is expressed as $C e^{(-l/5)}$, $l = 0, \cdots, 9$, where C is a constant used to make the total channel power unity. In the simulations of our SR-CFO estimation algorithm, the grid spacing is assumed to be 0.01, based on which we can find that $\bar{K} = 800$, when $Q = 8$ is assumed. In addition, in order to satisfy the constraint of $hw_i \geq |\eta_i|$ in (20) with a high probability, the probability of P_γ in (23) is chosen as 0.9999.

First, Figs. 1 and 2 show the MSE versus the SNR performance of the different CFO estimators, when $\epsilon_{\max} = 0.2$ (see Fig. 1) and $\epsilon_{\max} = 0.35$ (see Fig. 2), respectively. Here, $\epsilon_{\max}$ represents the maximum
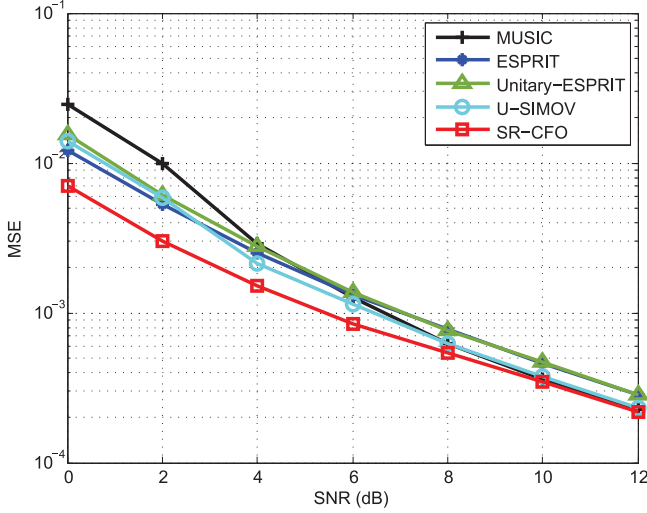
Fig. 1.   MSE versus SNR performance of the different CFO estimators under the parameters of $Q = 8$, $P = 128$, $K = 4$ and $\epsilon_{\max} = 0.2$.
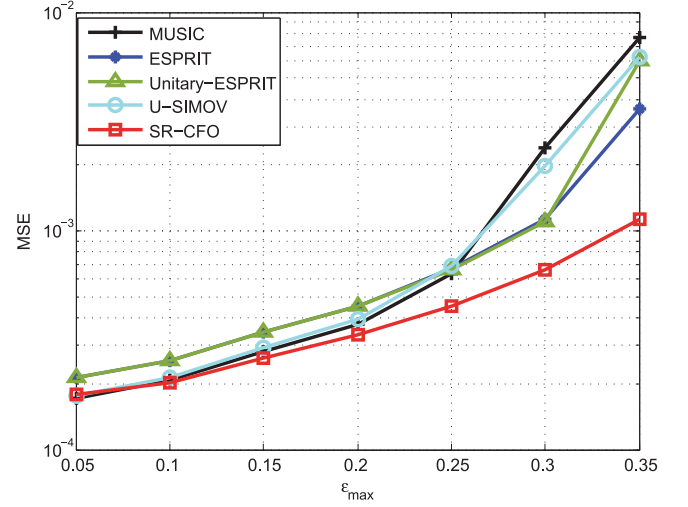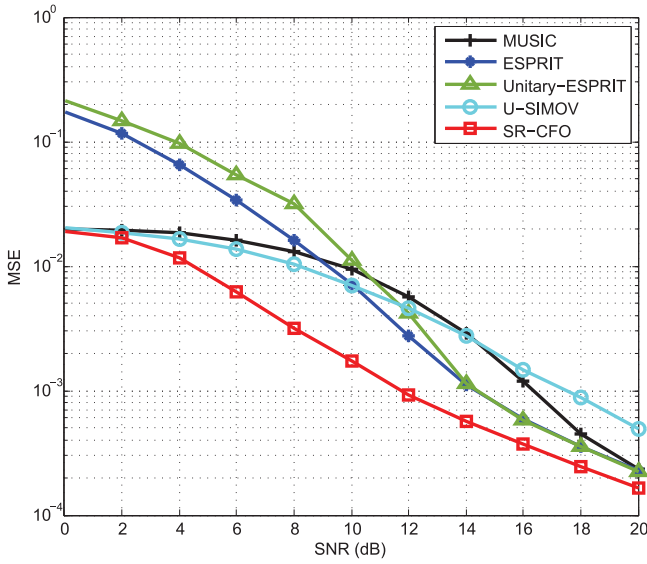

Fig. 3.   MSE versus $\epsilon_{\max}$ performance of the different CFO estimators, when the parameters of $Q = 8$, $P = 128$, $K = 4$ and SNR $= 12$ dB are used.

where $\lfloor \cdot \rfloor$ is a round down operator, $\hat{\epsilon}_m^{(k)}$ and $\hat{\theta}_m^{(k)}$ are the estimates to $\epsilon^{(k)}$ and $\theta^{(k)}$, respectively. Finally, for each realization in (B), $\{\hat{\theta}_m^{(k)}\}_{k=0}^{K-1}$ are given by the K largest local maximum of $\bar{\theta}^k$ selected by (12). For the purpose of comparison, in Figs. 1 and 2, four existing estimators are considered, which are the MUSIC [4], ESPRIT [5], Unitary-ESPRIT [6] and the U-SIMOV [7] algorithms.

From Figs. 1 and 2, we can explicitly observe that our proposed SR-CFO estimator outperforms the other considered estimators in terms of the MSE performance, especially when the effective CFOs are relatively large. This is due to the fact that our proposed SR-CFO estimator is designed based on sparse recovery, which is capable of providing finer resolution, even in the low SNR region, than the other CFO estimators.

Fig. 3 depicts the MSE versus $\epsilon_{\max}$ performance of the proposed and the other four estimators. Over the whole range of $\epsilon_{\max}$, the SR-CFO estimator outperforms the other estimators. As predicted, in comparison with the four existing estimators, the SR-CFO estimator becomes more significant, as $\epsilon_{\max}$ increases. Therefore, the SR-CFO estimator is more robust to the CFOs than the other considered estimators.

Fig. 4 plots the MSE of the different estimators against the number of active users. As the number of active users increases, the MSE performance of all the estimators degrades. When there are more than 4 active users, the estimation performance of both the ESPRIT and the Unitary-ESPRIT becomes very poor. This is because the dimension of the signal subspace used by these two estimators is smaller than that used by the other approaches. As shown in Fig. 4, our proposed SR-CFO estimator outperforms all the other estimators, provided that there are at least two active users.

Finally, the impact of the regularization parameter h on the MSE performance of the SR-CFO estimator is demonstrated in Fig. 5, when a range of SNR values are considered. In the figure, the h values evaluated by the approach provided in Section III-B are presented as red stars. As shown in the figure, the MSE obtained by these estimated h values is close to the minimum MSE achievable. Therefore, the regularization
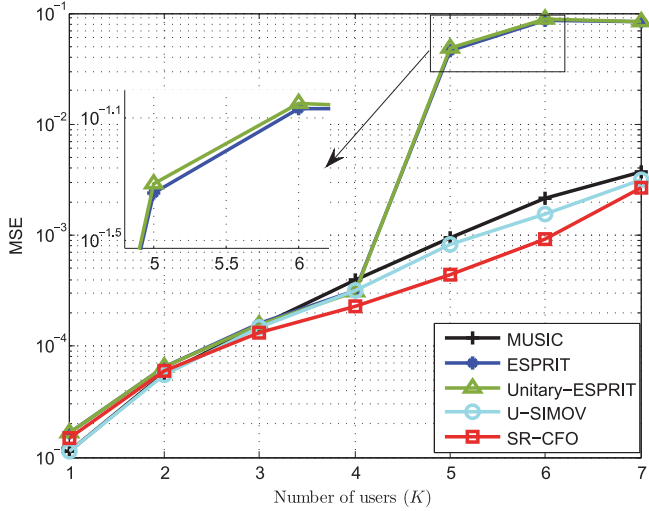

Fig. 2.   MSE versus SNR performance of the different CFO estimators under the parameters of $Q = 8$, $P = 128$, $K = 4$ and $\epsilon_{\max} = 0.35$.

absolute value of the effective CFOs, while the effective CFOs imposing on the different user signals follow the uniform distribution in $[-\epsilon_{\max}, \epsilon_{\max}]$. The MSE depicted in the figures is calculated by

$$\text{MSE} = \frac{1}{MK} \sum_{m=0}^{M-1} \sum_{k=0}^{K-1} (\hat{\epsilon}_m^{(k)} - \epsilon^{(k)})^2 \qquad \text{(A)}$$

where M is the number of realizations, and

$$\hat{\epsilon}_m^{(k)} = \hat{\theta}_m^{(k)} Q - \lfloor \hat{\theta}_m^{(k)} Q \rfloor \qquad \text{(B)}$$

Fig. 4. MSE versus the number of users for the different CFO estimators under the parameters of $Q = 8$, $P = 128$, $\epsilon_{\max} = 0.35$ and SNR=12 dB.
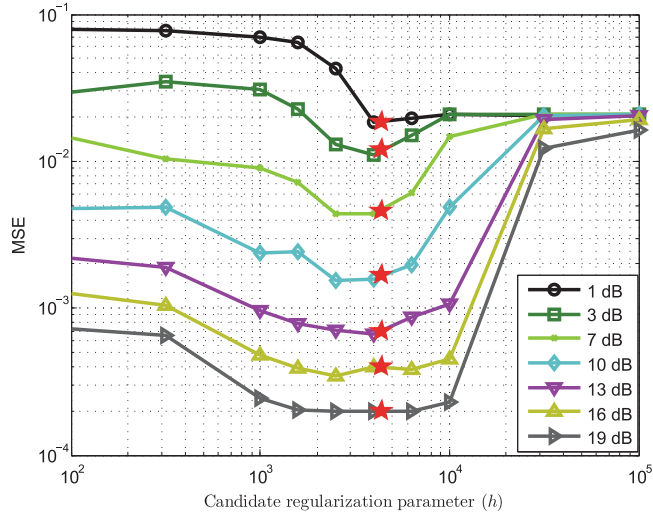

Fig. 5. Effect of regularization parameter on the MSE performance of the SR-CFO estimator with respect to different SNRs under the parameters of $Q = 8$, $P = 128$ and $\epsilon_{\max} = 0.35$.

parameter derived by our proposed approach in Section III-B is nearly optimum in terms of the minimum MSE.

V. CONCLUSION

A novel SR-CFO estimator without relying on pilots has been proposed and investigated against some existing estimators. In our sparse recovery problem, the selection matrix and whitening filter have been designed in order to mitigate the effect of noise and sampling error on the CFO estimation. Furthermore, an approach has been proposed

for deriving the regularization parameter, so that the CFO estimator is capable of achieving a good trade-off between the estimation resolution and the estimation performance. Finally, the performance of the proposed SR-CFO estimator has been demonstrated and compared with that of a range of existing CFO estimators. Our studies and simulation results show that the proposed SR-CFO estimator outperforms all the other estimators in terms of the reliability of estimation, but at the cost of an increased implementation complexity. Furthermore, the regularization parameter derived by our proposed approach is nearly optimum for achieving the minimum MSE of CFO estimation.

REFERENCES

[1] M. O. Pun, M. Morelli, and C.-C. J. Kuo, "Maximum-likelihood synchronization and channel estimation for the uplink of an OFDMA system," *IEEE Trans. Commun.*, vol. 54, no. 4, pp. 726–736, Apr. 2006.

[2] Y. Zeng and A. R. Leyman, "Pilot-based simplified ML and fast algorithm for frequency offset estimation in OFDMA uplink," *IEEE Trans. Veh. Technol.*, vol. 57, no. 3, pp. 1723–1732, May 2008.

[3] S. W. Keum, D. H. Kim, and H. M. Kim, "An improved frequency offset estimation based on companion matrix in multi-user uplink interleaved of DMA systems," *IEEE Signal Process. Lett.*, vol. 21, no. 4, pp. 409–413, Apr. 2014.

[4] Z. Cao, U. Tureli, and Y.-D. Yao, "Deterministic multiuser carrier-frequency offset estimation for interleaved OFDMA uplink," *IEEE Trans. Commun.*, vol. 52, no. 9, pp. 1585–1594, Sep. 2004.

[5] J. Lee, S. Lee, K.-J. Bang, S. Cha, and D. Hong, "Carrier frequency offset estimation using ESPRIT for interleaved OFDMA uplink systems," *IEEE Trans. Veh. Technol.*, vol. 56, no. 5, pp. 3227–3231, Sep. 2007.

[6] R. Du, J. Wang, and F. Liu, "Unitary-ESPRIT algorithm for carrier frequency offset estimation for interleaved OFDMA uplink systems," *Wireless Pers. Commun.*, vol. 69, no. 4, pp. 1615–1627, 2013.

[7] J. C. Chang, "Carrier frequency offset estimation using improved unitary minimum output variance approaches for interleaved OFDMA uplink systems," *Wireless Pers. Commun.*, vol. 85, no. 3, pp. 1081–1091, 2015.

[8] S. Boyd and L. Vandenberghe, *Convex Optimization*. Cambridge, U.K.: Cambridge Univ. Press, 2004.

[9] Z.-Q. He, Z.-P. Shi, L. Hunag, and H. C. So, "Underdetermined DOA estimation for wideband signals using robust sparse covariance fitting," *IEEE Signal Process. Lett.*, vol. 24, no. 4, pp. 435–439, Apr. 2015.

[10] S. D. Babacan, R. Molina, and A. K. Katsaggelos, "Bayesian compressive sensing using Laplace priors," *IEEE Trans. Image Process.*, vol. 19, no. 1, pp. 53–63, Jan. 2010.

[11] S. Chen, D. L. Donoho, and M. Saunders, "Atomic decomposition by basis pursuit," *SIAM J. Sci. Comput.*, vol. 20, no. 1, pp. 33–61, 1998.

[12] P. L. Fackler, "Notes on Matrix Calculus," North Carolina State Univ., Raleigh, NC, USA, Tech. Rep., 2005. [Online]. Available: http://www4.ncsu.edu/∼pfackler/MatCalc.pdf

[13] Z.-M. Liu, Z.-T. Huang, and Y.-Y. Zhou, "Sparsity-inducing direction finding for narrowband and wideband signals based on array covariance vectors," *IEEE Trans. Wireless Commun.*, vol. 12, no. 8, pp. 3896–3907, Aug. 2013.

[14] J. Fang, F.-Y. Wang, Y.-N. Shen, H.-B. Li, and R. Blum, "Super-resolution compressed sensing for line spectral estimation: An iterative reweighted approach," *IEEE Trans. Signal Process.*, vol. 64, no. 18, pp. 4649–4662, Sep. 2016.

[15] X. Xu, X. Wei, and Z. Ye, "DOA estimation based on sparse signal recovery utilizing weighted ℓ_1-norm penalty," *IEEE Signal Process. Lett.*, vol. 19, no. 3, pp. 155–158, Mar. 2012.

[16] J. Capon, "High resolution frequency wave number spectrum analysis," *Proc. IEEE*, vol. 57, no. 8, pp. 1408–1418, Aug. 1969.

[17] J. F. Sturm, "Using SeDuMi 1.02, a MATLAB toolbox for optimization over symmetric cones," *Optim. Method Softw.*, vol. 11, pp. 625–653, Aug. 1999.

[18] P. Apkarian, A. Nemirovski, A. Laub, and M. Chilali, *LMI Control Toolbox Users Guide*. Natick, MA, USA: The MathWorks Inc., 1995.